

Original Article

# Harnessing Artificial Intelligence for Improved Harmonic Reduction in Rectifier Systems: A Hybrid Power Filter Approach

S. Parthasarathy<sup>1</sup>, M. Ulagammai<sup>2</sup>

<sup>1</sup>Department of EEE, KLN College of Engineering, Madurai, Tamil Nadu, India.

<sup>2</sup>Department of Etech, SRM Institute of Science and Technology, Vadapalani, Chennai, Tamil Nadu, India.

<sup>2</sup>Corresponding Author : [ulagammaimeyyappan@gmail.com](mailto:ulagammaimeyyappan@gmail.com)

Received: 10 June 2025

Revised: 12 July 2025

Accepted: 11 August 2025

Published: 30 August 2025

**Abstract** - Power electronics-based electrical equipment is widely used across modern industrial sectors, offering advancements in energy conservation, efficiency, performance, and industrial needs. However, these devices-such as rectifiers, converters, inverters, Variable Frequency Drives (VFDs), Uninterruptible Power Supplies (UPS), furnaces, and other equipment-are categorized as non-linear loads, leading to waveform distortion in the electric power supply. This waveform distortion is a significant issue, causing Power Quality (PQ) problems in both power systems and local distribution networks. Total Harmonic Distortion (%THD) is a key metric for assessing the extent of harmonic pollution in an electrical system. The IEEE 519-2022 standard provides clear guidelines on voltage and current harmonic limits (%THDV and %THDI) based on system voltage levels. This study focuses on reducing harmonics produced by a three-phase rectifier through the implementation of a hybrid harmonic filter that integrates both passive and active components. To improve the effectiveness of the active filter, an Artificial Neural Network (ANN) is employed. Real-time measured data are used to train the ANN, resulting in better %THDI reduction. The article presents a performance analysis of the proposed active harmonic filter, hybrid harmonic filter, and ANN-trained hybrid harmonic filter. Testing and validation of the proposed hybrid harmonic filters are conducted using the MATLAB simulation platform.

**Keywords** - Artificial Neural Networks, Hybrid filters, Variable frequency drives, Total Harmonic Distortion, Harmonic filter.

## 1. Introduction

Ensuring high-quality power delivery is essential in modern electrical systems, requiring the supply to be stable, consistent, and free from distortion. Ideally, voltage and current waveforms should remain purely sinusoidal, maintaining specified frequency and amplitude levels for end-user applications. However, nonlinear loads commonly found in real-world systems often distort these ideal waveforms. This distortion is typically measured as Total Harmonic Distortion (THD), which occurs when the fundamental waveform is altered by the presence of harmonics-frequencies that are integer multiples of the fundamental.

Devices such as AC/DC converters, Variable Frequency Drives (VFDs), Uninterruptible Power Supplies (UPSs), arc furnaces, and certain types of lighting, like fluorescent lamps, are major contributors to harmonic distortion. Their switching operations result in current waveforms that deviate significantly from sinusoidal forms, leading to a non-linear relationship with the applied voltage. Such distortions can negatively impact system performance, causing issues like

overheating, insulation degradation, protection system malfunctions, and inaccurate metering.

Both passive and active filtering techniques are employed to address harmonic problems. Passive filters, while economical and effective for specific frequencies, have limitations including fixed compensation, possible resonance with the power system, and large physical size. In contrast, Active Power Filters (APFs) offer adaptive filtering capabilities, adjusting to varying harmonic conditions in real time, making them suitable for dynamic and complex load environments. However, their widespread adoption is limited by high implementation costs and complex control requirements [7, 8]. As a middle ground, hybrid filters combining active and passive components have emerged, providing improved filtering performance at a lower cost by sharing the harmonic compensation burden.

Despite these developments, a key research gap remains in active filters' accurate and adaptive control, especially under dynamic conditions involving fluctuating harmonic



content and system parameters. Traditional control methods struggle to generate accurate reference signals in such environments, leading to suboptimal compensation.

This study addresses this gap by proposing the integration of Artificial Neural Networks (ANNs) into the control strategy of a hybrid power filter. ANNs, known for their learning and generalization capabilities, are particularly effective for nonlinear, time-varying systems. The proposed ANN is trained using input parameters such as load power, firing angle, and current waveforms produced by a three-phase controlled rectifier functioning as a nonlinear load. The ANN calculates the essential gate signals to drive the active filter in real-time, confirming effective harmonic mitigation and power factor improvement under fluctuating operating environments [9-11].

This work presents a neural network-trained hybrid power filter with dual feedforward and feedback control, different from conventional passive and active filters with fixed compensation, which suffer from limited adaptability. Prevailing approaches frequently struggle under dynamic load and nonlinear conditions because of static control approaches. The proposed system integrates artificial intelligence to empower real-time learning and fine-tuning. This allows for more precise harmonic detection and flexible control than PID or fuzzy-based controllers described in previous studies. The approach addresses key stability, responsiveness, and scalability limitations found in traditional filtering techniques. The development and performance analysis of the planned system are carried out using MATLAB/SIMULINK, and its performance is assessed across diverse load conditions and firing angles, signifying its robustness and effectiveness in sustaining the power quality.

## 2. Proposed Hybrid Harmonic Filter for Non Linear Load

Hybrid power filters combine active and passive filtering elements, giving better filtering performance. This section of the study presents the hypothetical basis for the proposed active harmonic and hybrid power filtering approaches. Advances in switching technology and issues about the cost of passive filter components have stimulated research into active harmonic filters currently. Mostly at higher ratings, the cost of inductive and capacitive components can become exorbitant. Active filters outperform in challenging conditions where passive filters may fail, particularly in situations involving parallel resonance [13-15].

### 2.1. Active Harmonic Filter

Active filters alleviate harmonic distortions that occur due to nonlinear loads by injecting compensating current through power electronic devices. These filters are mainly used in low-voltage systems and depend on high-speed switching elements such as MOSFETs and IGBTs, because of their ability to withstand high currents and voltages while

switching rapidly. Active filters are preferred for their effective harmonic mitigation, small size, and adaptability.

Active filters are normally classified into two primary types: shunt and series configurations. Shunt active filters are commonly positioned at the load side and are primarily employed for eliminating current harmonics. They achieve this by injecting compensating currents that reflect the harmonic components in magnitude but are opposite in phase, effectively canceling both harmonic and reactive elements at the Point of Common Coupling (PCC) additionally, if series active filters are placed in line with the power supply through a coupling transformer to mitigate voltage harmonics by maintaining stable voltage levels at the load terminals.

To generate these compensating signals, active filters rely on converter circuits such as Voltage Source Inverters (VSIs) or Current Source Inverters (CSIs). In this study, a VSI-based shunt active filter is employed to suppress current harmonics.

As shown in Figure 1, the proposed shunt active filter incorporates a control system that continuously measures key electrical parameters, including source current, load current, and load voltage. Based on these real-time measurements, the controller produces gate signals that govern the inverter's switching, ensuring optimal filter performance.

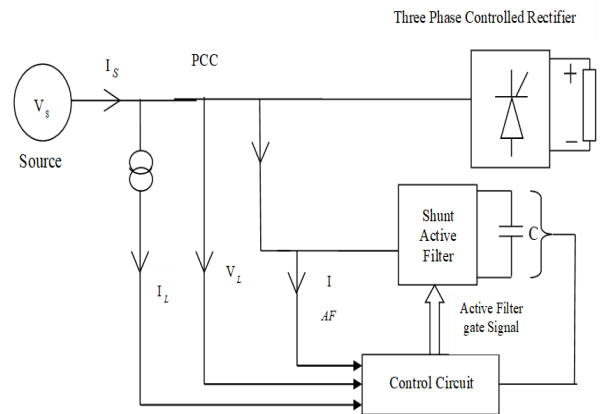


Fig. 1 Simplified schematic of the active filter setup

### 2.2. Control Technique of Active Harmonic Filter

The control mechanism for the active filter necessitates the computation of harmonic content within the load currents. Several methods exist for controlling active filters, including Instantaneous Reactive Power Theory, Fourier Transformation, and dq-Transformation. The dq-Transformation technique is employed in the proposed active filter. Space vector transformation is employed in this method to enable the identification and quantification of harmonics in non-sinusoidal current signals. Researchers typically utilize active filters with both feedforward and feedback control loops.

In feedforward control:

1. The control system acquires real-time measurements of the load current,  $i_L$ .
2. It then applies digital signal processing to isolate the harmonic portion from the total current.
3. To suppress the harmonic content, the active filter supplies a compensating current equal in magnitude but opposite in phase to that sourced from the supply voltage VS.

In feedback control:

1. Instantaneous supply current,  $I_s$ , is sensed by the control unit.
2. The harmonic portion of the supply current is extracted using digital signal processing algorithms.
3. A compensating voltage is applied by the active filter across the transformer's primary winding. When the feedback gain is sufficiently high, this effectively minimizes the harmonic current in the supply.

The feedback control strategy plays a vital role in directing harmonic components of the load current into the active filter, thereby preventing harmonic currents from the supply side from flowing into the filter. This targeted control enhances the performance of the passive filter by minimizing the risk of overloading and maintaining its filtering capability. Furthermore, feedback control allows the active filter to act like a damping resistor for lower-order harmonics, thus reducing potential resonance between the passive filter and the system's inductive elements. On the other hand, the feedforward control approach focuses on selectively extracting and mitigating specific harmonics-particularly the fifth harmonic-from the load current, guiding it into the active filter for mitigation. The control system employs the dq-transformation technique to precisely recognize and process distorted current signals. The major components of this approach include abc-to-dq and dq-to-abc transformations. Also, it uses a Phase Locked Loop (PLL) for synchronization, High Pass and Low Pass Filters (HPF and LPF), and a current-to-voltage conversion unit, as represented in Figure 2.

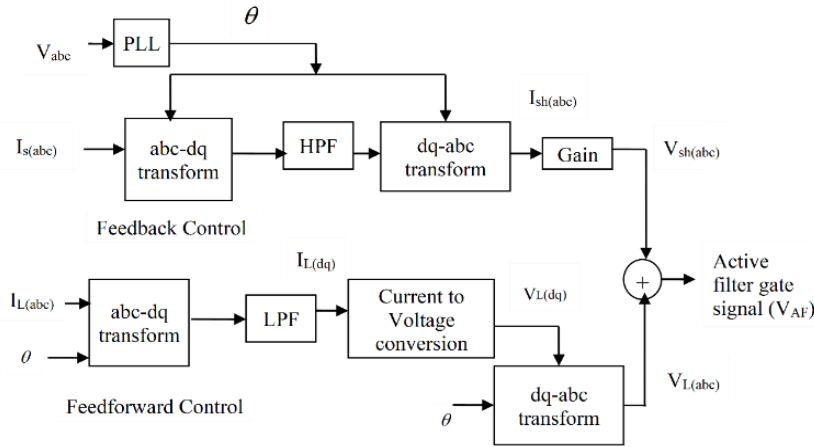


Fig. 2 Control scheme of active filter

In the dq-transformation technique, the time-dependent three-phase load currents  $I_L(abc)$  are initially captured within a stationary reference frame, and then the measured three-phase load currents are converted into a synchronously rotating dq reference frame associated with the fundamental frequency of the AC supply.

This transformation depends on the phase angle ( $\theta$ ), which is continuously traced by a Phase Locked Loop (PLL). Compared to the conventional P-Q theory, the dq-based method results in better signal decomposition and control precision.

In this frame, the abc-to-dq transformation equations are applied to convert the time-domain currents into direct-axis (d) and quadrature-axis (q) components. These dq signals can then be separated into their respective DC (fundamental) and AC (harmonic) parts for further analysis and control.

$$\begin{bmatrix} i_{Ld} \\ i_{Lq} \end{bmatrix} = \frac{2}{3} \begin{bmatrix} \cos \theta & \cos \left( \theta - \frac{2\pi}{3} \right) & \cos \left( \theta + \frac{2\pi}{3} \right) \\ \sin \theta & \sin \left( \theta - \frac{2\pi}{3} \right) & \sin \left( \theta + \frac{2\pi}{3} \right) \end{bmatrix} \begin{bmatrix} i_{La} \\ i_{Lb} \\ i_{Lc} \end{bmatrix} \quad (1)$$

abc to dq Transformation: Using a two-axis rotating reference frame, The abc-to-dq transformation translates three-phase signals into their equivalent components along the direct (d) and quadrature (q) axes in a rotating reference frame., q-axis, and zero-sequence components.

The voltage conversion from the three-phase (abc) system to the dq frame is carried out using Equations (2) to (4).

$$e_d = \left( \frac{2}{3} \right) \left[ \left( e_a \sin(\omega t) \right) + \left( e_b \sin \left( \omega t - \frac{2\pi}{3} \right) \right) + \left( e_c \sin \left( \omega t + \frac{2\pi}{3} \right) \right) \right] \quad (2)$$

$$e_q = \left(\frac{2}{3}\right) \left[ (e_a \cos(\omega t)) + \left( e_b \cos\left(\omega t - \frac{2\pi}{3}\right) \right) + \left( e_c \cos\left(\omega t + \frac{2\pi}{3}\right) \right) \right] \quad (3)$$

$$e_0 = \left(\frac{1}{3}\right) (e_a + e_b + e_c) \quad (4)$$

dq to abc Transformation: Reversing the Park transformation, the dq-to-abc conversion block translates the d-axis, q-axis, and zero-sequence signals-defined in a rotating reference frame-into their corresponding three-phase voltages. Equations (5) to (7) define this dq-to-abc voltage transformation.

$$e_a = e_d \sin(\omega t) + e_q \cos(\omega t) + e_0 \quad (5)$$

$$e_b = e_d \sin\left(\omega t - \frac{2\pi}{3}\right) + e_q \cos\left(\omega t - \frac{2\pi}{3}\right) + e_0 \quad (6)$$

$$e_c = e_d \sin\left(\omega t + \frac{2\pi}{3}\right) + e_q \cos\left(\omega t + \frac{2\pi}{3}\right) + e_0 \quad (7)$$

The dq-transformation method offers both advantages and disadvantages. While accurate tracking of source voltages ensures minimal impact of source voltage harmonics on filtering performance, this tracking necessitates increased computing power. The PLL serves a critical function in feedback control by dynamically adjusting the phase of a local signal to maintain synchronization with the external input signal. This PLL produces sine and cosine waveforms that are required for the abc to dq transformation technique.

Accurate determination of the phase angle ( $\theta$ ) of the source voltage is vital for synchronizing the reference signals with the voltage waveform. This synchronization is done by the Phase-Locked Loop (PLL), which locks onto the fundamental frequency of the supply voltage. The PLL effectively handles waveform distortions by ensuring consistent phase tracking.

A High-Pass Filter (HPF) enables high-frequency components to pass while attenuating frequencies below a specific cutoff point. Conversely, a Low-Pass Filter (LPF) allows only low-frequency signals to pass, filtering out components above its cutoff frequency. The degree of attenuation across frequencies depends on the design and characteristics of each filter.

For feedforward control, the conversion of current quantities into voltage quantities through real and reactive powers is indispensable. The conversion process involves transforming current components ( $i_{Ldq}$ ) into voltage components ( $v_{Ldq}$ ) using real and reactive power, as depicted in Equation (8).

$$\begin{bmatrix} P \\ Q \end{bmatrix} = \begin{bmatrix} e_d & e_q \\ -e_q & e_d \end{bmatrix} \begin{bmatrix} i_d \\ i_q \end{bmatrix} \quad (8)$$

As shown in Figure 2, the system's signal flow begins with the three-phase source voltage ( $V_{abc}$ ) being directed into the PLL block, which calculates the phase angle  $\theta$ . This angle serves as a reference for both abc-dq and dq-abc transformations. Simultaneously, these transformation blocks measure and utilise the source current and load current. In the feedback control loop, the current components are converted into voltage components using a gain block. Subsequently, the outputs of these two control loops are combined, resulting in the generation of the necessary gate pulses (VAF) for the active filter.

### 2.3. Hybrid Harmonic Filter

Active power filters effectively address the limitations of conventional passive filters, such as fixed compensation issues, resonance problems, and large size. However, their significant drawback lies in their high cost. Hybrid filters, which combine active and passive filtering elements, present a cost-effective alternative for power quality improvement. In this arrangement, a shunt-connected active filter protects the three-phase system by compensating for harmonic distortions and by addressing the reactive power requirements of the load. When connected in parallel with the utility source and the active filter, the passive filter helps ease the burden on the active filter. It does so by supplying a portion of the reactive power and filtering out specific harmonics. This synergy lowers the power rating and cost requirements of the active filter.

Hybrid filters incorporate power electronic switching components like MOSFETs, IGBTs, Thyristors, and GTOs alongside traditional passive components like inductors, capacitors, and resistors. The structural layout of a hybrid harmonic filter is illustrated in Figure 3.

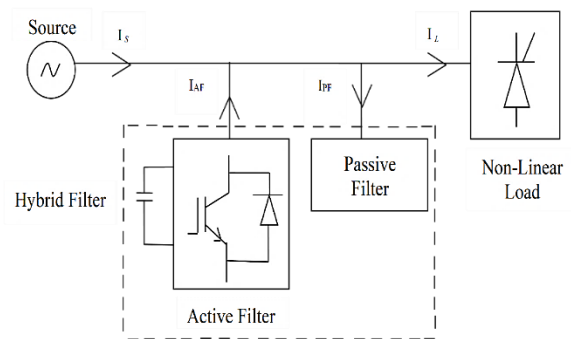


Fig. 3 Hybrid harmonic filter

Compared to purely active or passive filters, this hybrid configuration offers a more practical and economically viable solution, particularly in high-power applications. Key considerations in hybrid filter design include operational principles, system performance, and overall cost efficiency. An enhanced hybrid filter topology for rectifier-based loads



was proposed by Bhim Singh and Vishal Verma (2007). Connected in parallel with nonlinear loads, this system reroutes harmonic currents away from the supply lines and simultaneously improves the power factor while mitigating harmonic distortion.

### 3. Architecture of Neural Network

Artificial Neural Networks (ANNs) are algorithmic frameworks modeled after the structure and operation of the human brain, where multiple processing units operate concurrently. The behavior of the network is primarily governed by the strength of connections, referred to as weights, between these processing elements. Learning in ANNs involves adjusting these weights so that, for a given input, the network produces an output that closely approximates a desired target.

A widely used architecture is the two-layer feedforward neural network, which typically includes nonlinear activation functions, such as the sigmoid, that are typically employed in the hidden layers, while the output layer often uses a linear activation function to produce continuous outputs. In the current study, the ANN training is carried out using the Levenberg-Marquardt (LM) backpropagation algorithm. As Wilamowski and Yu (2010) noted, the LM algorithm offers an efficient and optimized approach to training by minimizing the mean squared error and is evaluated through regression metrics.

The Backpropagation (BP) learning algorithm updates the network’s weights based on error minimization, typically using gradient descent, to enhance classification or prediction performance. This method allows the network to iteratively learn and refine its internal parameters during training. A backpropagation neural network is composed of an input layer, one or more hidden layers, and an output layer. Neurons within the network apply nonlinear activation functions, allowing the model to capture intricate patterns and relationships between the input and output variables.

Additionally, neurons in the hidden and output layers incorporate bias terms-special units with fixed inputs-that function similarly to adjustable weights. Figure 4 presents the schematic of the backpropagation network used in this study, showing the directional flow of signals through ‘n’ input nodes, ‘p’ hidden neurons, and ‘m’ output neurons. The matrices V and W represent the weight connections from the input to hidden and hidden to output layers, respectively. Sivanandam and Deepa (2007) provided a comprehensive study of different neural network models. In contrast, Temurtas et al. (2004) implemented feedforward and Elman-type recurrent neural networks for harmonic detection within active filter frameworks, achieving enhanced processing efficiency and a simplified detection methodology.

$$y = \sigma(\omega_0 + \sum_{i=1}^k \omega_i x_i) \tag{9}$$

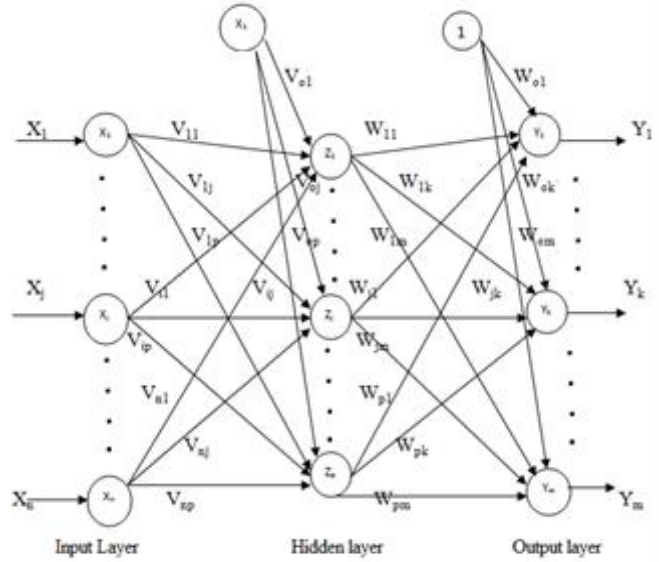


Fig. 4 Architecture of neural network

To enhance efficiency and achieve precise outputs, activation is applied, providing a driving force in attaining accurate results. Similarly, in Artificial Neural Networks (ANNs), activation functions are employed over the net input to compute the network's output. Various activation functions, such as Identity, Binary Step, Bipolar Step, Sigmoid, and Ramp function, serve this purpose.

Among these functions, the sigmoid function is extensively utilized in backpropagation networks due to its favorable relationship between function value and derivative value at a given point, reducing computational complexity during training. Also referred to as the log-sigmoid function, it can be defined using Equation (10), where  $\alpha$  represents the steepness parameter determining the function's behavior, as illustrated in Figure 5.

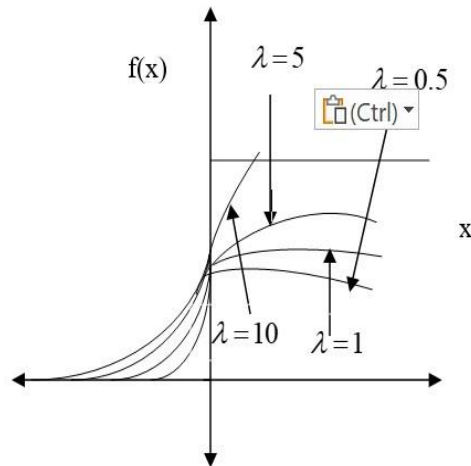


Fig. 5 Log-Sigmoid transfer function

The log-sigmoid activation function generates output values within the range of 0 to 1, corresponding to neuron inputs that vary from negative to positive infinity. This nonlinear function is commonly used in neural network models due to its smooth gradient and bounded output. Sivanandam and Deepa (2007) have examined several activation functions, including the log-sigmoid (equation 10), for their suitability in various neural network applications.

$$f(x) = \frac{1}{1+e^{-\lambda x}} \tag{10}$$

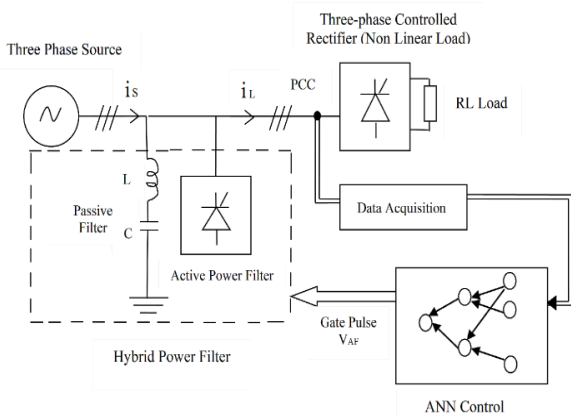


Fig. 6 Schematic diagram of the proposed ANN-controlled hybrid power filter

#### 4. Proposed ANN-Based Hybrid Power Filter

##### 4.1. System Description

Figure 6 presents the architectural layout of the proposed hybrid power filter system based on Artificial Neural Networks (ANN). In this configuration, a three-phase controlled rectifier functions as the nonlinear load. The hybrid filtering system integrates a shunt active filter with a tuned passive filter to mitigate power quality issues. Key electrical parameters-namely, the three-phase source, source current and load current, which corresponds to the rectifier input current-are captured through a data acquisition system. These signals are processed to generate gate control signals for the active filter.

The control strategy can be executed using two distinct approaches: a feedforward control scheme aimed at filtering harmonic currents, and a feedback control scheme for managing harmonic voltages. Both methods rely on the abc-to-dq transformation, which converts three-phase sinusoidal signals into direct-axis (d), quadrature-axis (q), and zero-sequence components within a rotating reference frame. The Phase-Locked Loop (PLL) plays a key role by continuously adjusting the phase of a locally generated signal to synchronize with the input signal, thereby enabling precise gate signal generation for the active filter. A high-pass filter is employed to extract the harmonic components from the current by attenuating the fundamental frequency and passing

higher-frequency signals. This study chooses a three-phase controlled rectifier as the representative nonlinear load. Its load characteristics are obtained from real-time data collected at the Point of Common Coupling (PCC) of a Variable Frequency Drive (VFD), using a power quality analyzer. This real-world load profile is used to validate the simulation model of the proposed ANN-driven hybrid power filter. Figure 7 presents real-time screenshots of the three-phase VFD measurements for reference.

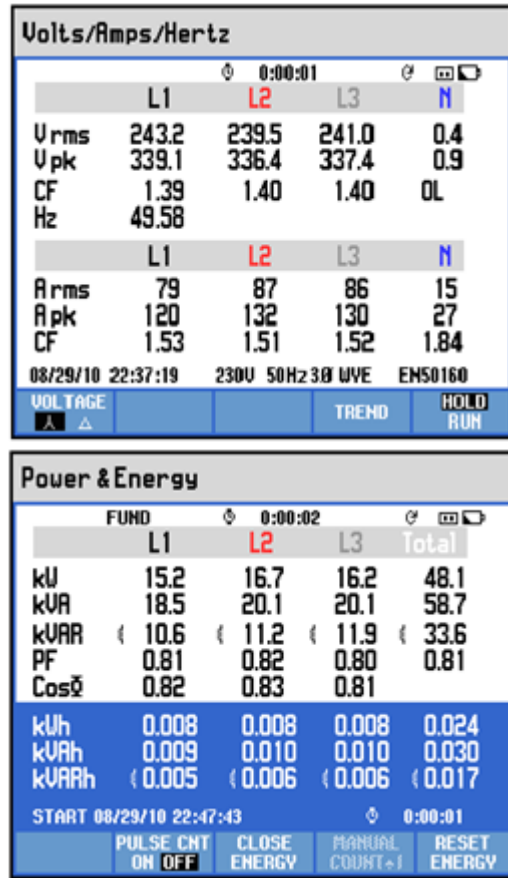


Fig. 7 Real-time data for a VFD

The data collection, network creation, training the network and performance analysis are the sequential processes of NN to get the desired output. They are discussed in the following section.

##### 4.2. Data Collection

The data collection and preparation phase is a crucial step in network design. Multilayer networks can achieve robust generalization within the bounds of the training data. For the proposed ANN model, four input parameters are considered: the rectifier firing angle ( $\alpha$ ), load real power (P), source current (IS), and load current (IL).

Data are gathered based on the variation of the firing angle from 1° to 50° with a step interval of 1°, and the load

real power ranging from 10kW to 50kW with a step interval of 3kW. For each scenario, the source current, load current, and network output are recorded. In this study, the network output is designated as the target, representing the gate control signal for the active filter. In total, 1,400 samples are to be collected and normalized. Increasing the number of samples contributes to an efficient training process.

#### 4.3. Network Creation

While two-layer feedforward networks have the potential to learn nearly any input-output relationship, adding more layers to a feedforward network may enable it to learn complex relationships more efficiently. Typically, it's advisable to begin with two layers and then consider increasing to three layers if the performance with two layers is unsatisfactory. Mark Hudson Beale et al (2010) have provided insights into the creation, training, and testing procedures of neural networks using various NN toolbox approaches.

The Artificial Neural Network (ANN) employed in this work utilizes a three-layer architecture comprising four input neurons, a hidden layer with twenty neurons, and one output neuron, as illustrated in Figure 8. Several network configurations were evaluated, and the structure with twenty hidden neurons yielded the best performance. The network's output is responsible for generating the gate control signals required to operate the active power filter. The selection of input and output neurons is inherently tied to the specifics of the application. While increasing the number of neurons in the hidden layer can enhance the network's capacity to model complex relationships, it may also result in increased computational load and a higher risk of overfitting.

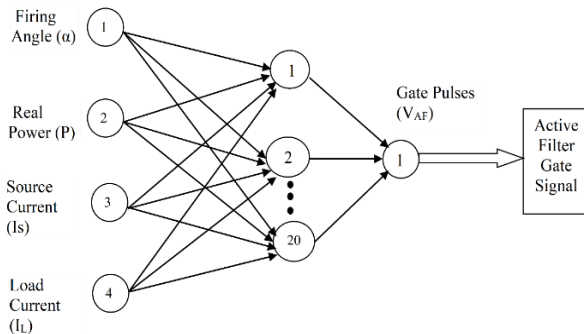


Fig. 8 Architecture of the proposed ANN model

Training a neural network entails fine-tuning its weights and biases to enhance its predictive accuracy. In feedforward networks, the Mean Squared Error (MSE) is a performance metric used for evaluation. It determines the average of the squared errors between the predicted outputs and the required target values, thus giving the prediction accuracy. Neural network training is done under two modes: incremental and batch. In incremental (or online) mode, after each individual input is presented, the network weights are updated. But in

batch mode, the weights are updated only after the entire training dataset is processed. For multilayer feedforward networks, the Backpropagation (BP) algorithm is mostly preferred to minimise mean squared error. This algorithm fine-tunes the weights and biases using the negative gradient of the cost function (Loss function), ensuring error reduction.

The learning rate controls the magnitude of weight adjustment during each training step, with values typically ranging from 0 to 1. An acceleration factor can be added to the weight updating process to accelerate the rate of convergence. The acceleration factor makes significant weight adjustments until corrections are aligned for multiple patterns of data.

The Neural Network Toolbox has multiple training algorithms that include different factors such as the task convergence, training data size, network architecture, target error levels, and the application-whether it comes under pattern recognition or function approximation. For function approximation tasks that involve networks with an optimum number of weights, the Levenberg-Marquardt (LM) algorithm is commonly preferred because of its rapid convergence and better accuracy in lessening mean squared error. Due to its efficiency and precision, the LM algorithm is a suitable choice for estimating the performance of the proposed three-layer neural network in this study.

The Levenberg-Marquardt algorithm-trained Neural network is well-suited for curtailing nonlinear least squares problems, resulting in rapid convergence for medium-sized neural networks. Training data for this network is obtained by simulating the system without an ANN under various load conditions and firing angles ( $\alpha$ ) of controlled rectifiers. Source currents ( $I_s$ ), load currents ( $I_L$ ), and corresponding gate pulses of the active filter are recorded. These parameters act as inputs for the ANN model, with gate pulses as the desired targets to train the proposed ANN.

#### 4.4. Performance Analysis

After providing inputs and targets in the MATLAB NN toolbox, the training process begins. It generates plots for performance, training state, and regression. The performance plot displays the variation of the error function throughout the training process, indicating how well the network performs on the training, validation, and test sets. The training state plot provides insights into essential metrics such as gradient values and validation checks, which help assess convergence and guide training termination.

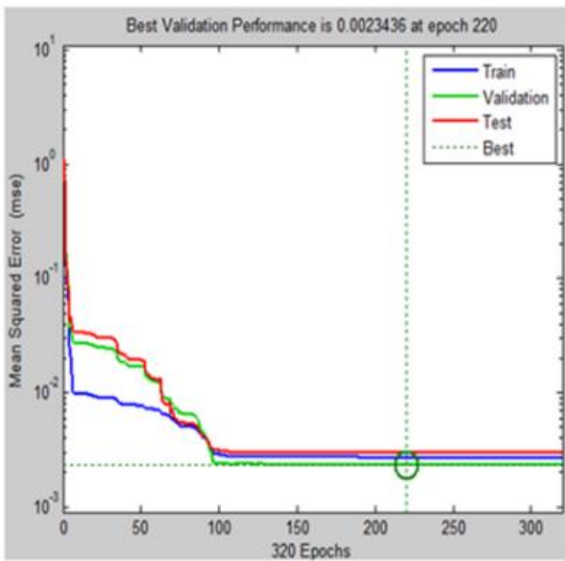
Additionally, regression plots visualize the correlation between predicted outputs and actual targets, which may not align perfectly due to inherent real-world data variability. The performance and regression graphs, serving as training indicators, are depicted in Figure 9 for Phase A. The performance plot juxtaposes training, validation, and testing data performances against the best output derived from mean

squared error evaluation. In this instance, 320 iterations and 100 validation checks yield the optimal outcome. Notably, the performance plot in Figure 9(a) highlights the peak validation at epoch 220. In the regression graph, the Regression (R) values quantify the correlation between network outputs and targets. For Phase A, the overall regression stands at 0.93042, as illustrated in Figure 9(b). This metric reflects the cumulative regression across training, validation, and testing datasets, providing insight into model performance.

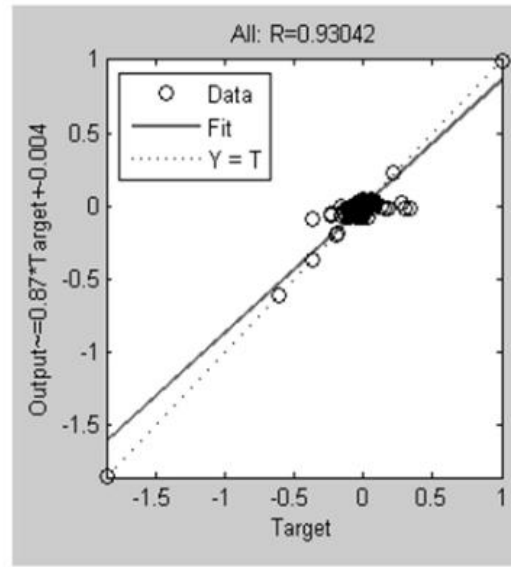
In Phase B, the training process completes 457 iterations to fulfil the 100 validation checks. Figures 10(a) and 10(b) display the performance and regression plots, respectively.

Notably, both the validation and test curves exhibit similar trends, with the best validation performance observed at the 457th epoch, as depicted in Figure 10(a). The overall regression for Phase B stands at 0.92722, as illustrated in Figure 10(b). For Phase C, the ANN model undergoes 303 iterations. The optimal validation performance for Phase C is achieved at the 203rd epoch, as shown in Figure 11(a).

Moreover, the complete regression result for Phase C is obtained as 0.93108, as depicted in Figure 11(b). The training, testing, and validation plots exhibit minimal deviation, suggesting low error discrepancies between training and testing phases.

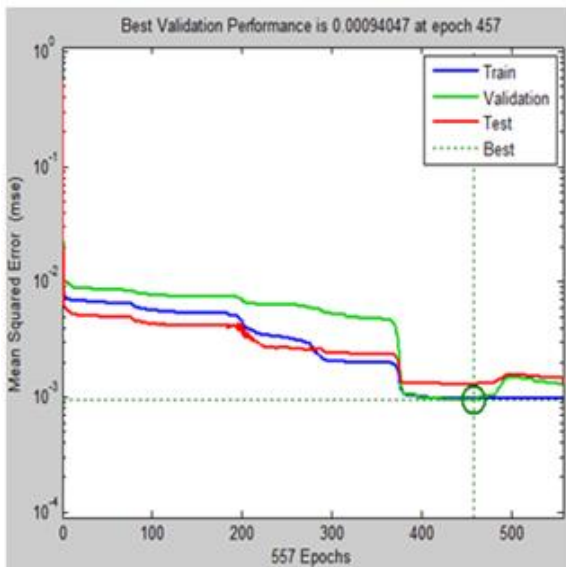


(a)

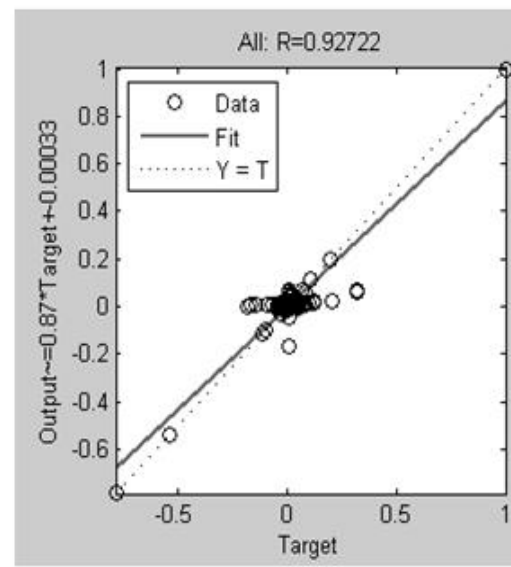


(b)

Fig. 9 ANN trained performance and regression plots for phase A (a) Performance graph, and (b) Regression graph.



(a)



(b)

Fig. 10 ANN trained performance and regression plots for phase B (a) Performance graph, and (b) Regression graph.



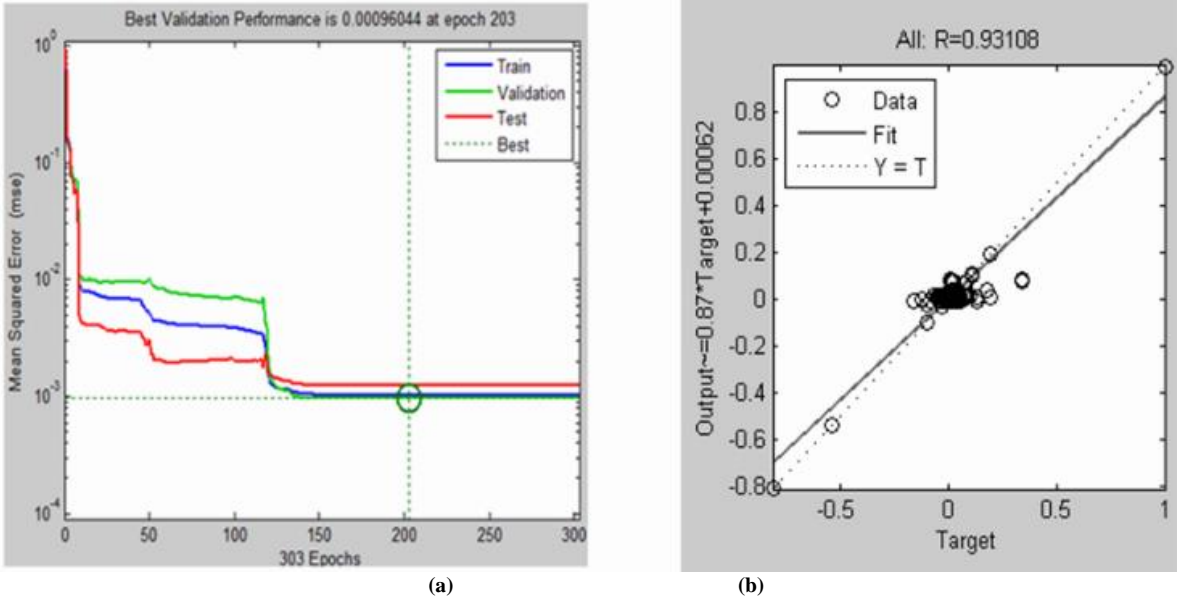


Fig. 11 ANN trained performance and regression plots for phase C (a) Performance graph, and (b) Regression graph.

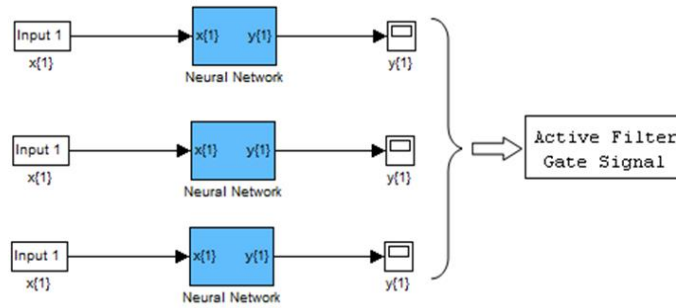


Fig. 12 ANN Simulated models for respective phases

After training the network using Neural Network Toolbox, the simulation model was developed, as shown in Figure 12. During the period of training, weights are updated in the ANN model, which gives a minimized error. The trained ANN model has been tested using simulation, until getting minimized Total Current Harmonic Distortion (THDI) specified by IEEE standard 519-1992.

## 5. Results and Discussion

In this section, the simulation models and their corresponding results for the system under various scenarios are analyzed, focusing on different firing angles and load powers. Specifically, the analysis centers on a firing angle ( $\alpha$ ) of  $30^\circ$ . To evaluate the effectiveness of the system, the Total Harmonic Distortion of the Current (THDI) is examined. A comparative analysis is conducted by simulating the system both with and without the filter.

### 5.1. Analysis without Filter

The simulation model depicting the system without a harmonic filter is shown in Figure 13. A three-phase source supplies power to a controlled rectifier, which acts as a non-

linear load, via a three-phase step-down transformer. The six-pulse rectifier, constituting six valves, represents the non-linear load subsystem. An RL load is connected to the DC output side of the rectifier, with the load power details provided in Figure 13. The controlled rectifier generates harmonic distortion based on its firing angle and load profile variation. The distorted input current waveform of the rectifier is observed through the scope. Furthermore, the input current waveforms of the rectifier and the harmonic spectrum, along with THDI values, are obtained using Fast Fourier Transform (FFT) within the Powergui block, available in MATLAB SIMULINK. The Powergui block in MATLAB/SIMULINK is used to analyze the harmonic spectrum of current waveforms. Figure 14 shows the unfiltered current waveform and its harmonic spectrum, where the 3<sup>rd</sup> and 5<sup>th</sup> harmonic components dominate. At a firing angle of  $30^\circ$ , the Total Harmonic Distortion (THD) values are 18.39% for Phase A, 19.20% for Phase B, and 18.84% for Phase C. These exceed the permissible THD limits set by the IEEE 519-1992 standard, which recommends a current THD of  $\leq 5\%$ . High THD leads to overheating, power losses, and reduced equipment lifespan.

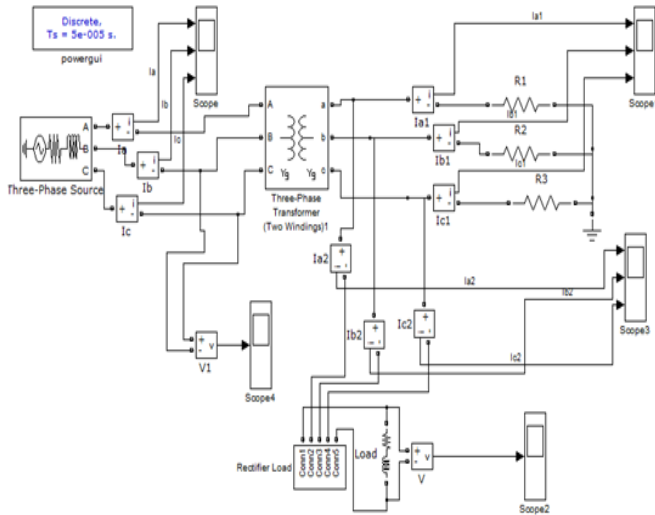


Fig. 13 Simulation model: six pulse rectifier without harmonic filter

Passive filters can reduce specific harmonic frequencies but suffer from limitations such as resonance and fixed compensation. Active filters offer better dynamic compensation but are costly and require complex control systems. To overcome these drawbacks, a hybrid harmonic filter is proposed, integrating both passive and active filtering techniques. The passive component is tuned to suppress prominent low-order harmonics, while the active filter targets higher-order and dynamically varying harmonic components. This synergy reduces the required rating and associated cost of the active filter and enhances the system's overall harmonic mitigation capability. Furthermore, the hybrid configuration demonstrates superior adaptability under fluctuating load conditions. Simulation results confirm the effectiveness and robustness of the proposed solution, showing a significant reduction in THD. Compliance with IEEE standards is achieved. Thus, the hybrid filter improves power quality efficiently and economically.

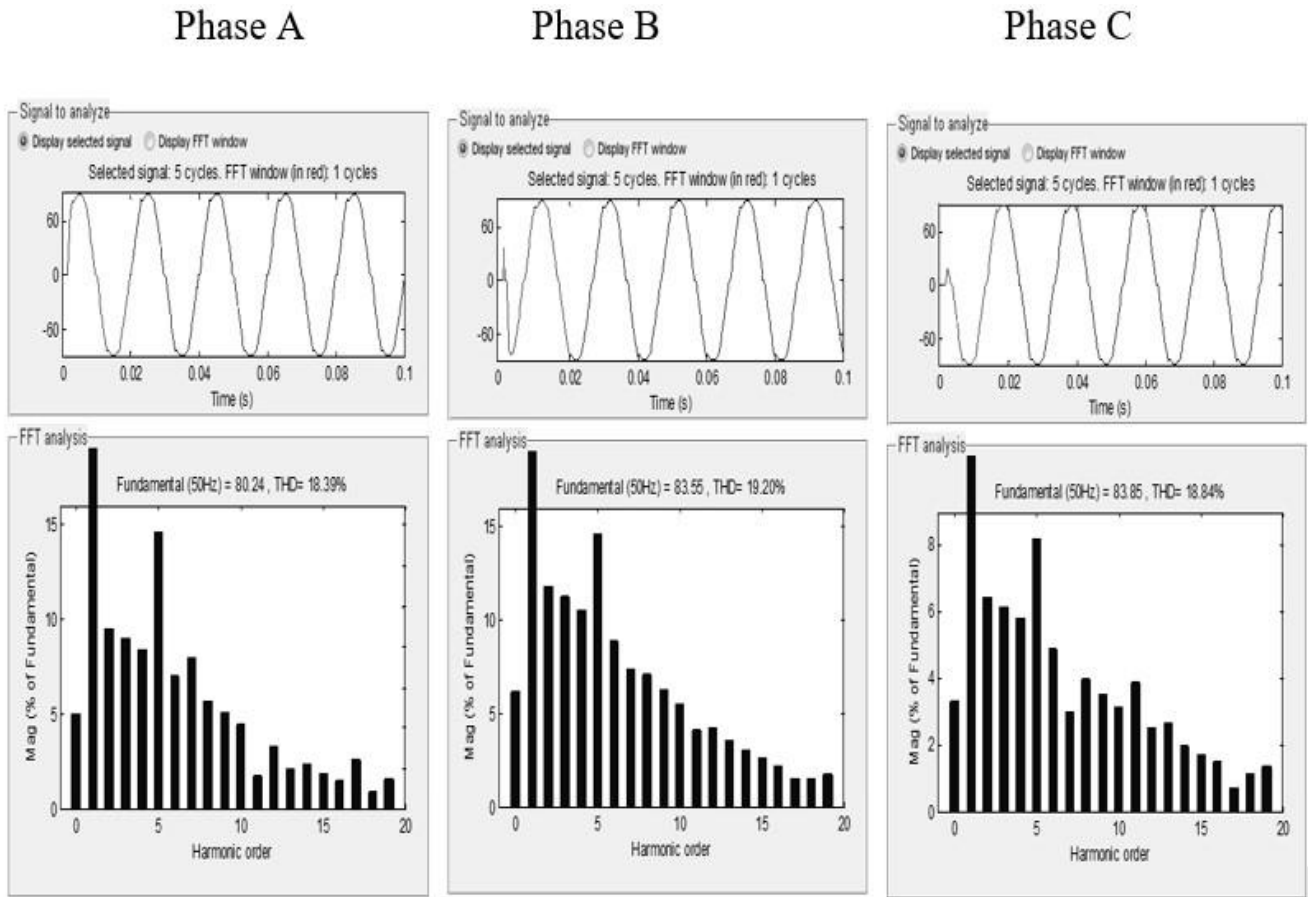


Fig. 14 Rectifier input current waveforms (s) and harmonic spectrum without filter

### 5.2. Analysis with ANN Trained Hybrid Power Filter

A shunt-connected hybrid power filter, integrating both passive and active elements, is implemented to mitigate harmonic distortion on the input side of a three-phase controlled rectifier. Initial analysis conducted through the Powergui block reveals that the 3<sup>rd</sup> and 5<sup>th</sup> harmonic orders are

the most significant contributors to waveform distortion. Tune passive filters are designed to mitigate these specific harmonic frequencies. The design procedure, based on Equations (8) to (14), incorporates system power ratings, and the final values of passive filter components are listed in Table 1.

**Table 1. Design values of passive filter parameters**

Order of Harmonics	Inductance (mH)	Capacitance (µF)
3 <sup>rd</sup>	1.01	1114
5 <sup>th</sup>	0.33	1228

In dynamic loading scenarios, passive filters alone are insufficient due to their fixed tuning. To enhance filtering performance, passive filters are paired with an active harmonic filter, forming a hybrid configuration where the active part's effectiveness is closely tied to its control approach, which generates precise gate pulses based on system conditions.

To enhance the control system, an Artificial Neural Network (ANN) is trained using key system parameters. The trained ANN provides real-time gate signals for the active filter, improving harmonic elimination under variable conditions. The ANN model, once validated, is implemented in the simulation environment (Figure 15), where it functions as a control subsystem for the hybrid filter system.

Simulation results in Figure 16 show that with the ANN-trained hybrid filter, THDI is significantly reduced to 4.20%, 4.68%, and 4.51% for Phase A, Phase B, and Phase C, respectively. These values fall well within IEEE 519-1992 limits and reflect improved waveform quality.

Beyond harmonic mitigation, power factor improvement is achieved. According to Equation (11), power factor (PF) is inversely related to THDI. High harmonic content leads to phase misalignment between voltage and current. As given in Table 2, the system's power factor improves to 0.999 with the ANN-controlled hybrid filter, compared to ~0.982 without filtering.

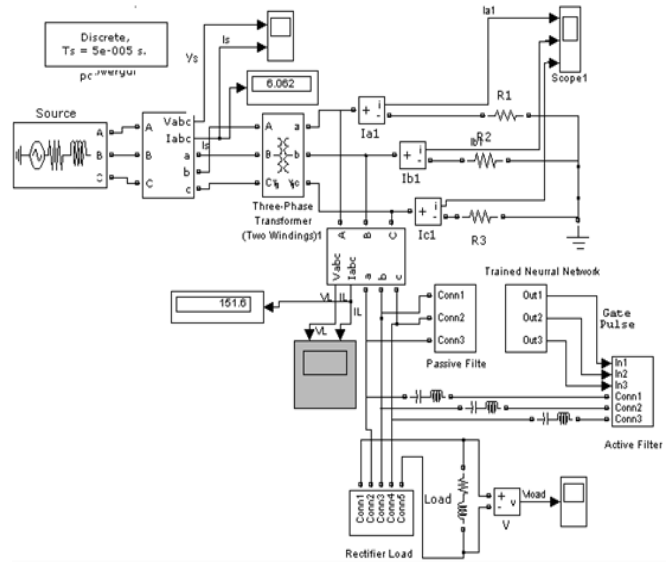


**Fig. 15 Simulation model with an ANN-trained hybrid power filter for rectifier**

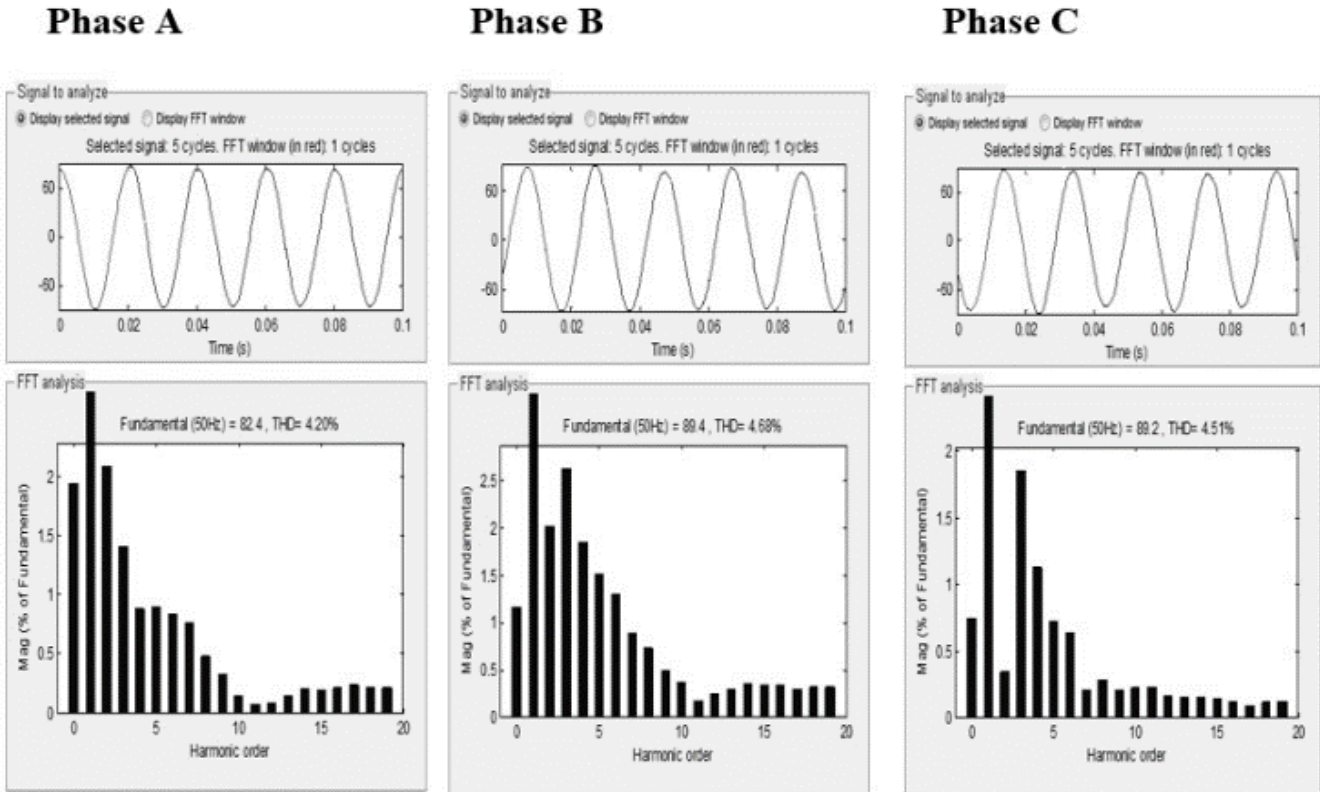


**Fig. 16 Rectifier input current waveforms and harmonic spectrum with an ANN-trained hybrid power filter**

**Table 2.** Comparison of THDI and power factor for controlled rectifier without and with a neural-trained hybrid power filter

Phase	Rectifier Firing Angle = 30°			
	Without Filter		With Neural Trained HPF	
	THDI (%)	Power Factor	THDI (%)	Power Factor
Phase A	18.39	0.983	4.20	0.999
Phase B	19.20	0.982	4.68	0.999
Phase C	18.84	0.982	4.51	0.999

In addition to reducing harmonic distortion, harmonic filters aid in improving the power factor, a key parameter reflecting the system's power quality and efficiency. As emphasized by Azazi H.Z. et al. (2010), various topologies of Power Factor Correction (PFC) circuits exist, each offering specific advantages and limitations depending on system requirements. Equation (11) defines the mathematical relationship between the system power factor and the Total Harmonic Distortion Index (THDI), highlighting the inverse correlation between harmonic content and the quality of current waveform alignment with voltage.

When THDI is high, the current waveform is significantly distorted and deviates from the voltage waveform, resulting in a lagging or leading power factor. Such deviations from unity (i.e., a power factor of 1) introduce multiple operational issues: increased I<sup>2</sup>R losses, reduced system efficiency, heating of equipment, and the potential injection of harmonics into the neutral conductor. These harmonics can interfere with the performance of other connected equipment and disrupt sensitive loads. The primary goal of any power factor correction technique is to reduce waveform distortion and ensure that the current waveform closely aligns with the voltage waveform, tracks the voltage waveform as accurately as possible, thereby reducing reactive power and enhancing overall power transfer capability.

$$PF = \frac{1}{\sqrt{1 + \left(\frac{THDI(\%)}{100}\right)^2}} \quad (11)$$

By significantly reducing current harmonics through the application of an intelligent filtering approach—such as the neural network-trained Hybrid Power Filter (HPF)—the system power factor can be brought closer to unity. To validate this, simulation results for a controlled rectifier operating with a firing angle of 30° were analyzed and compared for different filter configurations. Table 2 presents the THDI and power factor values for the system without any filter, and with the implementation of the ANN-based HPF. The results clearly indicate that the ANN-trained hybrid filter offers superior performance. Without filtering, the THDI for phases A, B, and

C stands at 18.39%, 19.20%, and 18.84%, respectively, with corresponding power factors of 0.983, 0.982, and 0.982.

Upon integrating the ANN-based HPF, the THDI is reduced to 4.20%, 4.68%, and 4.51%, and the power factor is remarkably improved to 0.999 for all three phases. This substantial enhancement ensures compliance with IEEE 519-1992 standards and improves the sinusoidal purity of the input current waveform, which now closely resembles an ideal sine wave. These improvements collectively contribute to reduced energy losses, enhanced voltage stability, and improved performance of connected electrical and electronic equipment.

### 5.3. Performance Analysis of Proposed Filter

In this study, the load power of the controlled rectifier is varied systematically from 10 kW to 50 kW to comprehensively evaluate the effectiveness of the proposed filtering strategies under realistic and dynamic operating conditions. Unlike many existing works that evaluate filter performance at fixed load levels, this investigation emphasizes a load-dependent analysis, which adds practical relevance to the study. For each load level, the corresponding Total Harmonic Distortion Index (THDI) is recorded for different configurations—without a filter, with a conventional hybrid filter, and with the proposed neural network-trained hybrid power filter (ANN-HPF). The comparative results are visually presented using a bar chart in Figure 17, which distinctly demonstrates the consistent and superior harmonic mitigation capability of the ANN-HPF across the entire load range. The novelty of this approach lies in the adaptive learning mechanism of the ANN, which dynamically adjusts the active filter control based on varying load and system conditions, unlike fixed-rule or PID-based controllers used in earlier works. A performance effectiveness metric is introduced to quantitatively evaluate the impact of the filtering system. This metric measures the percentage reduction in the current harmonic distortion of the supply before and after the application of the filter. The performance coefficient, expressed in Equation (12), serves as an indicator of harmonic mitigation efficiency for each filter setup. Among different tested structures, the proposed ANN-based Hybrid Power Filter (ANN-HPF) is highly effective under various load conditions. The proposed system is highly adaptable and robust. The proposed system's performance, which was experimentally confirmed through improved filtering performance under dynamic load conditions, enhances its practical suitability for modern power systems that integrate nonlinear and time-variant loads.

$$\varepsilon_i = \left[1 - \left(\frac{I_d}{I_{do}}\right)\right] * 100 \quad (12)$$

Hybrid Power Filter, Active Filter, and Neural Trained Hybrid Filter implement distinct methods that differ in efficiency with respect to Total Harmonic Distortion Index (THDI). Filter performance in reducing the Total Harmonic



Distortion Index (THDI) for the three filtering methods is shown in the bar chart with respect to the increase in load from 10 kW to 50 kW. The neural-trained filter performed the best in all load scenarios, maintaining a THDI of 4.8%-5.2%, even as the load increased. THDI values of 6% to 6.8% from the hybrid filter indicate a medium performance where only partial and stable harmonic suppression was achieved. The active filter is the least efficient among all three filters, with the highest THDI of 9%-11% across all load scenarios. These

results show that the adaptation of the ANN-based hybrid filter to the changing dynamic conditions of operation is quite effective. It can actively learn to accurately adjust for the harmonic distortion in factors such as the load profile, which makes dynamic compensation possible, unlike the static compensation of the other two filters. Thus, the performance of the ANN-trained hybrid filter is shown to be more effective and increases the efficiency of power quality in non-linear power systems.

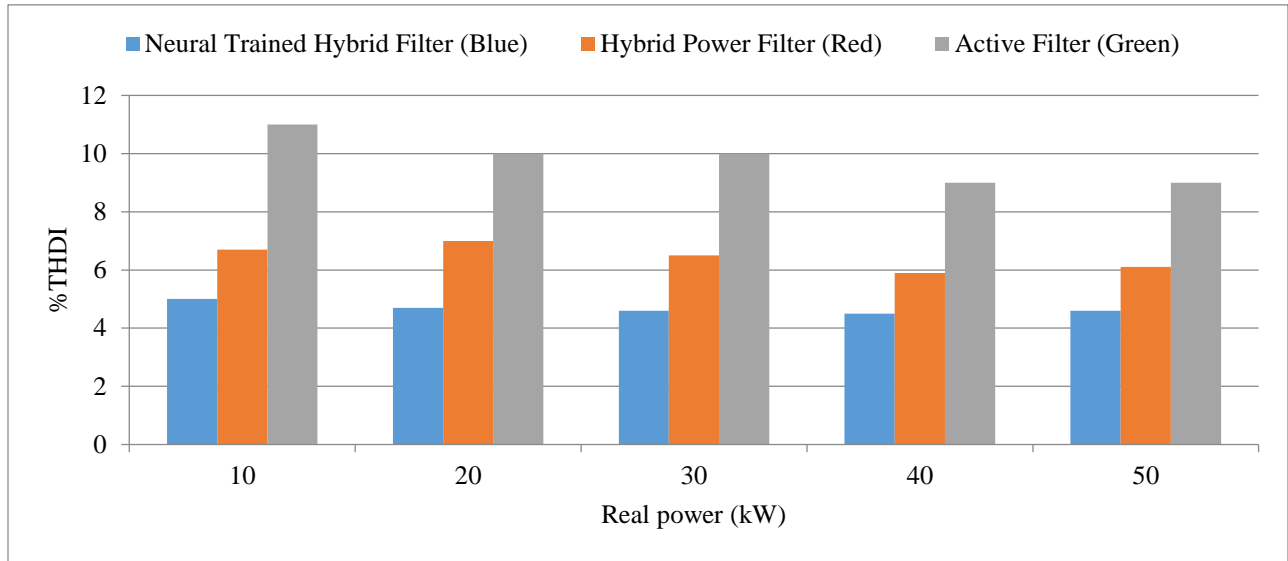


Fig. 17 Comparison of % THDI vs. Real power

The above bar chart compares the % filter effectiveness across Phase A, Phase B, and Phase C for the above-discussed filter types. Neural Trained Hybrid Filter reliably gives better efficiency, reaching nearly 98% in Phases A and C, and around 95% in Phase B. The Active Filter exhibits the lowest filter performance at 85% to 90%. The Hybrid Power Filter

performs reasonably well, achieving effectiveness scores between 93% and 96% across all phases. These results prove that the ANN-based hybrid filter gives better harmonic suppression in all phases. This adaptive learning ability ensures reliable performance under varying load conditions, outperforming traditional filtering methods.

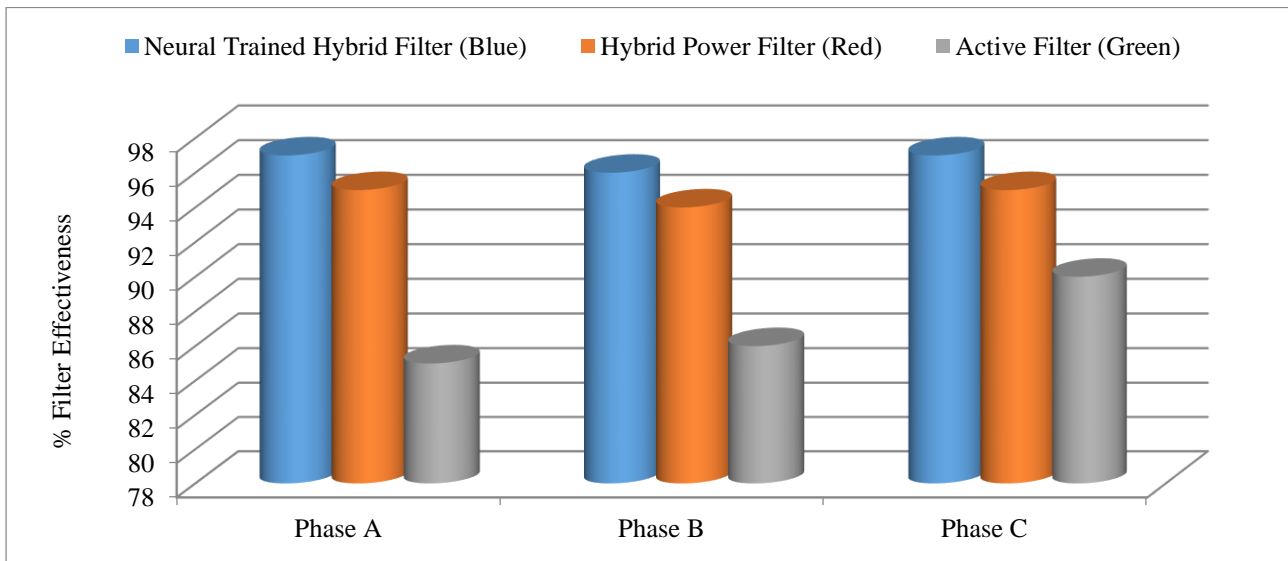


Fig. 18 Effectiveness of filter performance

## 6. Conclusion

This study presents a novel ANN-trained hybrid power filter designed to reduce current harmonics and improve the power factor in a nonlinear three-phase rectifier system operating under varying load conditions (10 kW to 50 kW) and firing angles. Unlike conventional filters, the proposed system integrates both feedforward and feedback control schemes, enabling dynamic real-time control through neural network learning. This dual-control architecture enhances adaptability and responsiveness, addressing the limitations of fixed-parameter filters. Simulation results demonstrate a significant reduction in Total Harmonic Distortion (THD): for

instance, Phase A THD decreased from 18.39% (unfiltered) to 4.20% with the ANN-based filter, while the power factor improved from 0.983 to 0.999.

Additionally, filter effectiveness surpassed 97% in all phases, outperforming traditional active and hybrid filters by 8–12%. These quantitative outcomes affirm the superiority and novelty of the ANN-based hybrid filter in achieving IEEE 519-1992 compliance and optimizing power quality. In conclusion, the proposed method offers an intelligent, cost-effective, and scalable solution for harmonic mitigation in dynamically varying power systems.

## References

- [1] P. Acharjee, and S.K. Goswami, "Expert Algorithm Based on Adaptive Particle Swarm Optimization for Power Flow Analysis," *Expert Systems with Applications*, vol. 36, no. 3, pp. 5151-5156, 2009. [[CrossRef](#)] [[Google Scholar](#)] [[Publisher Link](#)]
- [2] Khaled Djerboub et al., "Particle Swarm Optimization Trained Artificial Neural Network to Control Shunt Active Power Filter Based on Multilevel Flying Capacitor Inverter," *European Journal of Electrical Engineering*, vol. 22, no. 3, pp. 199-207, 2020. [[CrossRef](#)] [[Google Scholar](#)] [[Publisher Link](#)]
- [3] H. Akagi, "Modern Active Filters and Traditional Passive Filters," *Bulletin of the Polish Academy of Sciences: Technical Sciences*, vol. 54, no. 3, pp. 255-269, 2006. [[Google Scholar](#)] [[Publisher Link](#)]
- [4] Alexander Kusko, *Power Quality in Electrical Systems*, McGraw-Hill Education, 2007. [[Google Scholar](#)] [[Publisher Link](#)]
- [5] Ali M. Eltamaly, "A Modified Harmonics Reduction Technique for a Three-Phase Controlled Converter," *IEEE Transactions on Industrial Electronics*, vol. 55, no. 3, pp. 1190-1197, 2008. [[CrossRef](#)] [[Google Scholar](#)] [[Publisher Link](#)]
- [6] Ali M. Eltamaly, "A Novel Harmonic Reduction Technique for Controlled Converter by Third Harmonic Current Injection," *Electric Power Systems Research*, vol. 91, pp. 104-112, 2012. [[CrossRef](#)] [[Google Scholar](#)] [[Publisher Link](#)]
- [7] Arindam Maitra, S. Mark Halpin, and Christopher A. Litton, "Application of Harmonic Limits at Wholesale Points of Delivery," *IEEE Transactions on Power Delivery*, vol. 22, no. 1, pp. 263-269, 2007. [[CrossRef](#)] [[Google Scholar](#)] [[Publisher Link](#)]
- [8] Jos Arrillaga, and Neville R. Watson, *Power System Harmonics*, John Wiley & Sons, Ltd, 2003. [[CrossRef](#)] [[Google Scholar](#)] [[Publisher Link](#)]
- [9] A.Y. Hatata, M. Eladawy, and K. Shebl, "Parameter Control Scheme for Active Power Filter Based on NARX Neural Network," *WSEAS Transactions on Power Systems*, vol. 13, pp. 118-124, 2018. [[Google Scholar](#)] [[Publisher Link](#)]
- [10] Barry W. Kennedy, *Power Quality Primer*, McGraw-Hill Education, 2000. [[Google Scholar](#)] [[Publisher Link](#)]
- [11] B. Singh, K. Al-Haddad, and A. Chandra, "A Review of Active Filters for Power Quality Improvement," *IEEE Transactions on Industrial Electronics*, vol. 46, no. 5, pp. 960-971, 1999. [[CrossRef](#)] [[Google Scholar](#)] [[Publisher Link](#)]
- [12] F. Temurtas et al., "Harmonic Detection Using Feed Forward and Recurrent Neural Networks for Active Filters," *Electric Power Systems Research*, vol. 72, no. 1, pp. 33-40, 2004. [[CrossRef](#)] [[Google Scholar](#)] [[Publisher Link](#)]
- [13] M.H.J. Bollen, "What is Power Quality?," *Electric Power Systems Research*, vol. 66, no. 1, pp. 5-14, 2003. [[CrossRef](#)] [[Google Scholar](#)] [[Publisher Link](#)]
- [14] Chia-Nan Ko, Ying-Pin Chang, and Chia-Ju Wu, "A PSO Method with Nonlinear Time-Varying Evolution for Optimal Design of Harmonic Filters," *IEEE Transactions on Power Systems*, vol. 24, no. 1, pp. 437-444, 2009. [[CrossRef](#)] [[Google Scholar](#)] [[Publisher Link](#)]
- [15] Chih-Ju Chou et al., "Optimal Planning of Large Passive-Harmonic Filters Set at High Voltage Level," *IEEE Transactions on Power Systems*, vol. 15, no. 1, pp. 433-441, 2000. [[CrossRef](#)] [[Google Scholar](#)] [[Publisher Link](#)]
- [16] Swati Gade and Rahul Agrawal, "Optimal utilization of unified power quality conditioner using the JAYA optimization algorithm," *Engineering Optimization*, vol. 55, no.1, pp. 1–18, 2023. [[CrossRef](#)] [[Google Scholar](#)] [[Publisher Link](#)]